

Document downloaded from:

<http://hdl.handle.net/10251/161869>

This paper must be cited as:

Martínez-Gimeno, MA.; Jiménez Bello, MA.; Lidón, A.; Manzano Juarez, J.; Badal, E.; Pérez-Pérez, JG.; Bonet, L.... (2020). Mandarin irrigation scheduling by means of frequency domain reflectometry soil moisture monitoring. *Agricultural Water Management*. 235:1-9.  
<https://doi.org/10.1016/j.agwat.2020.106151>



The final publication is available at

<https://doi.org/10.1016/j.agwat.2020.106151>

Copyright Elsevier

Additional Information

# Mandarin irrigation scheduling by means of frequency domain reflectometry soil moisture monitoring

M.A. Martínez-Gimeno<sup>1,2</sup>, M.A. Jiménez-Bello<sup>3</sup>, A. Lidón<sup>3</sup>, J. Manzano<sup>4</sup>, E. Badal<sup>2</sup>, J.G. Pérez-Pérez<sup>2</sup>, L. Bonet<sup>2</sup>, D.S. Intrigliolo<sup>1,2</sup>, A. Esteban<sup>2,5</sup>

<sup>1</sup>Center for Applied Biology and Soil Sciences (CEBAS), Spanish National Research Council (CSIC) Murcia, Spain; <sup>2</sup>Valencian Institute for Agricultural Research (IVIA), Unidad Asociada al CSIC “Riego en la agricultura mediterránea” Valencia, Spain; <sup>3</sup>Research Institute of Water and Environmental Engineering, Polytechnic University of Valencia (IIAMA - UPV), Valencia, Spain; <sup>4</sup>Valencian Centre for Irrigation Studies, Polytechnic University of Valencia (CVER - UPV) Valencia, Spain. Spain; <sup>5</sup>School of engineering and architecture, University of Zaragoza (UNIZAR), Zaragoza, Spain.

## Abstract

The accurate estimation of plant water needs is the first step for achieving high crop water productivity. The main objective of the work was to develop an irrigation scheduling procedure for mandarin orchards under Mediterranean conditions based on replacing the amount of consumed water using reference values of soil moisture according to different phenological periods. The proposed methodology includes a definition part where the threshold values were established relating the trees' stem water potential and the volumetric soil water content measured with Frequency Domain Reflectometry probes. A second part includes the steps for standardizing measurements from capacitance probes by using the LEACHM hydrological simulation model to take into account the sensor-to-sensor variations. Finally, an extrapolation procedure based on soil water retention curves was used for adapting critical soil water content thresholds to different soil conditions.

27 Field evaluations were made in a citrus orchard located in eastern Spain during two  
28 seasons. Standardized critical soil water contents were: i) 24% vol. for post-harvest,  
29 bloom - fruit set and phase III of fruit growth; ii) 27% vol. for phase I of fruit growth, and  
30 iii) 29% vol. for phase II of fruit growth with average daily air vapour pressure deficit  
31 values ranging between 0.2 - 0.4; 0.9 - 1.1 and 1.1 - 1.3 kPa, respectively. When  
32 implemented in the orchard, the sensor-based strategy resulted in water saving of 26%  
33 respect to a control treatment, irrigated using the standard FAO-56 approach, without  
34 significant differences in yield and increasing the crop water productivity by 33%. In  
35 conclusion, we suggest that the determination and use of the critical soil water content is  
36 a useful tool for scheduling irrigation. The proposed standardization and extrapolation  
37 methodology allows the irrigation strategy to be applied to other mandarin orchards under  
38 similar climatic conditions.

39

## 40 **1. Introduction**

41 In arid and semi-arid zones, irrigated agriculture is the main user of water resources,  
42 reaching a proportion that could exceed 70–80% of the total water abstractions (Feres  
43 and Soriano, 2006). Citrus trees are widely cultivated in south-eastern Spain, where the  
44 predominant climate conditions are those typical of a semi-arid zones.

45 Climate change forecasts an increase in crop water requirements (CWR) and  
46 probably more severe drought periods (Menenti et al., 2013). Some scenarios for 2050  
47 predict 30-50% decrease of fresh water availability, while its demand on eastern and  
48 southern areas could be doubled (Milano et al., 2013).

49 In citrus trees, irrigation is essential to guarantee high quality and yield, and an  
50 effective water management strategy is crucial to cope with this situation of water scarcity  
51 (Garcia-Tejero et al., 2011) and avoid environmental hazards such as groundwater

52 pollution by nitrogen fertilizers (Quiñones et al., 2007). Precision irrigation aims to  
53 minimize water losses due to deep percolation during the watering events through  
54 increasing the efficiency of systems and using a schedule methodology based on the water  
55 exchange in the soil-plant-atmosphere system (Pérez, 2016).

56 Nowadays, the most widely used system for calculating irrigation needs is based on  
57 the water balance proposed in FAO paper number 56 (Allen et al., 1998). This method  
58 determines the CWR considering the reference evapotranspiration ( $ET_0$ ) and the crop  
59 coefficients ( $K_c$ ). Although some studies have adapted the FAO-56 algorithm for  
60 irrigation scheduling (Rallo et al., 2011), this strategy has some uncertainty calculating  
61 water needs for instance when tree light interception (Consoli et al., 2006) or crop load  
62 (Syvertsen et al., 2003; Yonemoto et al., 2004) change over the seasons. Therefore, a  
63 substantial improvement in irrigation management can be achieved if soil and plant water  
64 status are used for scheduling irrigation in woody perennial crops.

65 Indirect methods for monitoring soil water status are based on measuring soil matric  
66 potential ( $\Psi_{soil}$ ) or volumetric water content ( $\theta$ ) (Campbell and Campbell, 1982).  
67 Amongst the wide range of available devices, probes based on Frequency Domain  
68 Reflectometry (FDR) are nowadays the most widely used tools to determine the  $\theta$  because  
69 of their relatively affordable price and ease of use (Fares and Polyakov, 2006). Accuracy  
70 of obtained information depends on the probe installation (Evetts et al., 2002) which  
71 should minimize air gaps between the plastic shell and the soil. Under these  
72 circumstances, the accuracy of the FDR sensors can reach values of  $\pm 1\%$  vol. with soil  
73 specific calibration (Muñoz-Carpena et al., 2004). However, Provenzano et al. (2015)  
74 found higher differences in a capacitance probe calibration for a range of soils with  
75 different particle size distributions. The field practices used, and particularly those related  
76 with the orchard soil management that affects bulk density and organic matter content,

77 can play a significant effect on soil properties invalidating the calibration (Hignett and  
78 Evett, 2008; Paraskevas et al., 2012). When absolute  $\theta$  values are used for scheduling  
79 irrigation, using manufacturer default calibration equations might result in inappropriate  
80  $\theta$  estimations, and a site-specific analysis should be then performed (Evett et al., 2006).

81 Hydrological simulation could be an alternative tool for calibrating FDR probes and  
82 obtaining accurate  $\theta$  values. The Leaching Estimation And Chemistry Model (LEACHM)  
83 is a one-dimensional deterministic model that describes the water and solutes regimes in  
84 unsaturated or partially saturated soils (Hutson, 2003). LEACHM model has been widely  
85 used for simulating water, nitrogen, salts and pesticide behavior in soils (Ramos and  
86 Carbonell 1991; Asada et al., 2013; Nasri et al., 2015; Deng et al., 2017). The model has  
87 been used to evaluate water and nitrogen management in citrus orchards (Lidón et al.,  
88 1999; Alva et al., 2006; Lidón et al., 2013). It is a mechanistic model that uses the  
89 Richards equation (Richards, 1931) to simulate soil moisture variation, being as valid as  
90 other agro-hydrological models like SPAW, FAO, SMCR, SIMODIS and Hydrus 2D  
91 among others (Minacapilli et al., 2008, Zhang et al., 2010; Rallo et al., 2011; Autovino et  
92 al., 2018).

93 The usefulness of capacitance probes for scheduling irrigation can be increased if  
94 plants water status is included. This information integrates the effects of surrounding  
95 environmental conditions and the fraction of the water available in the soil for the plant  
96 (Moriani et al., 2012). In this sense, midday stem water potential ( $\Psi_{Stem}$ ) is considered  
97 as a benchmark indicator of the degree of plant water stress (Ruiz-Sánchez et al., 2010;  
98 Ballester et al., 2011). This indicator is obtained through a destructive measurement,  
99 which is time-consuming and needs dedication and currently it is impossible to automate.  
100 However, these measurements can play an essential role for irrigation scheduling when

101 comparing it with a reference value, corresponding to an ideal plant water status with full  
102 water availability (Spinelli et al., 2017).

103 The aim of the research was to develop an irrigation scheduling strategy for mandarin  
104 orchards under Mediterranean conditions based on replacing the amount of consumed  
105 water using reference values of soil moisture at different phenological periods. Threshold  
106 values to start irrigation were determined using relationships between  $\Psi_{Stem}$  and the  
107 volumetric soil water content measured with FDR probes ( $\theta_{FDR}$ ). The methodology  
108 includes a procedure for standardizing soil moisture capacitance probes readings and  
109 extrapolating scheduling thresholds for plots with different soil characteristics.

110

## 111 **2. Materials and methods**

### 112 ***2.1. General approach***

113 The methodology followed for scheduling mandarin irrigation by means of the  
114 proposed sensor-based strategy comprises three steps: definition, standardization and  
115 extrapolation.

116 The goal of the definition phase is to obtain a reference  $\theta$  for scheduling irrigation  
117 with FDR probes ensuring an adequate plant water status. The critical soil water content  
118 threshold ( $\theta_{crit-FDR}$ ) is defined from simultaneous measurements of  $\theta_{FDR}$  and  $\Psi_{Stem}$  in  
119 different periods of the crop cycle in which irrigation was withheld.

120 Secondly, the aim of the standardization phase was to gauge FDR probes minimizing  
121 sensor-to-sensor variations for scheduling irrigation with absolute critical soil water  
122 content ( $\theta_{crit}$ ) values. This step is needed considering that FDR probes might provide for  
123 different readings at the same moisture levels due to lack of calibration. The chosen  
124 methodology consists in comparing the soil water content obtained by means of a

125 hydrological simulation software ( $\theta_{SIM}$ ) with the  $\theta_{FDR}$  and computing the differences  
126 with a standardization equation.

127 And thirdly, in the extrapolation phase, a methodology based on soil water retention  
128 curves (SWRC) and the  $\Psi_{soil}$  was used for adapting  $\theta_{crit}$  to different soil physical  
129 conditions. The aim of these two last steps (standardization and extrapolation) are  
130 fundamental for applying the sensor-based strategy to other mandarin orchards located  
131 under similar climatic conditions.

## 132 **2.2. Experimental plot**

133 The study was carried out during 2015 and 2016 in a commercial citrus orchard  
134 located in Alberic in the south of the province of Valencia, Spain (39° 7' 31.33" N, 0° 33'  
135 17.06" W, 37 m a.m.s.l). The experiment was performed on mature 'Arrufatina' mandarin  
136 (*Citrus clementina* Hort. ex Tan.) trees grafted onto 'Carrizo' citrange (*Citrus sinensis*  
137 Osb. × *Poncirus trifoliata* Raf.) rootstock, with a tree spacing of 5.50 m × 4.25 m. Soil  
138 textural class, according to the USDA classification, is loam to sandy clay loam with  
139 percentages of clay ranging from 22 to 34% within the orchard. Soil organic matter was  
140 on average 1.3%. The climate is semi-arid with warm winters and dry summers with  
141 average annual precipitation of 400 mm, lower than the  $ET_0$ , 1000 - 1300 mm (IGN,  
142 2018). The plot was equipped with a drip irrigation system, automatic control valves and  
143 flow meters to monitor the amount of water applied. Water was supplied by two drip  
144 laterals with a total 7 emitters per tree (2.2 L h<sup>-1</sup> AZUD Premier PC AS (Azud,  
145 Alcantarilla, Murcia, Spain). Emitters were spaced at 1.2 m apart.

146 FDR water-content-profile probes (EnviroScan, Sentek, Stepney, Australia) were  
147 used for monitoring  $\theta_{FDR}$  at 0.2, 0.3 and 0.5 m depths where roots are mainly concentrated  
148 (Abouatallah et al., 2012) at 30 minutes time-step. A total of 6 FDR probes were installed  
149 in the experimental plot. Four probes (noted as Definition (Def) 1 to 4) were installed on

150 four contiguous trees used for establishing the  $\theta_{crit-FDR}$  thresholds. Two additional  
151 probes (noted as Validation (Val) 1 and 2) were installed under different trees for  
152 implementing the sensor-based strategy. All probes were located adjacent to the drip  
153 irrigation line and at about 0.10 m from the emitter following the installations  
154 recommendations by Bonet et al., (2010).

155 In order to characterize the soils where the 6 FDR probes were installed, two  
156 undisturbed soil cores (0.05 m height and 0.05 m diameter) were collected around the  
157 access tubes at 0.2, 0.3 and 0.4 m depths. Soil organic matter content (Walkley and Black,  
158 1934), dry bulk density and soil textural class according USDA classification (Soil  
159 Survey Staff, 1975) were determined.

### 160 **2.3. Critical soil water content definition.**

161 The  $\theta_{crit-FDR}$  below which plant water stress occurs, and it is necessary to start  
162 irrigation, was obtained by solving linear equations fed with simultaneous measurements  
163 of  $\Psi_{Stem}$  and  $\theta_{FDR}$ . Values of  $\Psi_{Stem}$  obtained in previous research carried out in the area  
164 for solving these equations (Ballester et al., 2014; Martínez-Gimeno et al. 2018) were  
165 adapted. The onset of plant water stress was established at -0.8 to -1.0 MPa from mid-  
166 September to May and at -1.0 to -1.2 MPa from June to mid-September. Measurements  
167 were made during three drought cycles in two consecutive years. Irrigation was withheld  
168 from May 4<sup>th</sup> to May 17<sup>th</sup> [days of the year (DOY) 124–137, period A1], July 20<sup>th</sup> to July  
169 26<sup>th</sup> (DOY 201–207, period B1) and November 12<sup>th</sup> to January 11<sup>th</sup> (DOY 316–11, period  
170 C1) in 2015–2016; and May 19<sup>th</sup> to June 8<sup>th</sup> (DOY 140–160, period A2), August 5<sup>th</sup> to  
171 August 19<sup>th</sup> (DOY 218–232, period B2) and December 1<sup>st</sup> to January 13<sup>th</sup> (DOY 336–13,  
172 period C2) in 2016-2017. According to common phenological stages of ‘Clementina  
173 arrufatina’ under climatic conditions of Mediterranean area along the season, period A  
174 corresponds with phase I of fruit growth, period B with phase II of fruit growth and period



175 C with phase III of fruit growth, bloom and fruit set and post-harvest. Definition probes  
176 1 to 4 were used for measuring the  $\theta_{FDR}$  during these periods. The  $\Psi_{stem}$  was measured  
177 in the same four trees equipped with the FDR probes by using a Schölander pressure  
178 chamber (Model 600, PMS Instrument Co., USA). Measurements were carried out with  
179 high frequency (from daily to weekly) during the drought cycles. For each tree,  
180 measurements were made on two leaves that were covered with aluminum foil bags at  
181 least one hour before the measurements (Turner, 1981). Average air vapour pressure  
182 deficit (VPD) was estimated for each drought cycle.

#### 183 **2.4. Critical soil water content standardization**

184 The adjustment to take into account sensor-to-sensor variation for using the  $\theta_{crit}$  with  
185 any FDR probe was made by contrasting  $\theta_{SIM}$  and  $\theta_{FDR}$ . Differences were quantified by  
186 solving the linear regression equation expressed as:

$$187 \theta_{FDR} = a\theta_{SIM} + b \quad [1]$$

188 where a and b are fitting parameters.

189 The LEACHM model was used for obtaining  $\theta_{SIM}$ . Input data includes soil physical  
190 and chemical properties of the different soil layers (texture, organic matter, bulk density,  
191 water retention parameters), plant data (crop cycle data, crop cover fraction) and weather  
192 (rain, temperature, thermal amplitude, potential evapotranspiration). The LEACHM  
193 model follows the method proposed by Childs and Hanks (1975) to calculate the  $ET_0$   
194 from the weekly reference evapotranspiration. The partition between evaporation and  
195 transpiration is made according to the crop cover fraction and following the equation  
196 proposed by Nimah and Hanks (1973).

197 The soil profile where FDR probes were installed was divided into several horizontal  
198 segments. The total simulation period was divided into short time intervals, and equations  
199 were solved for each soil layer and each water flow interval, which should be 0.1 day or

200 less. It was necessary to know the relations between hydraulic conductivity,  $\theta$  and  $\Psi_{soil}$ .  
 201 Those are based on the moisture retention function (Eq. 2) and the unsaturated hydraulic  
 202 conductivity function (Eq. 3) proposed by Campbell (1974) integrating the modification  
 203 suggested by Hutson and Cass (1987):

$$204 \quad \Psi_{soil} = a \left( \frac{\theta}{\theta_s} \right)^{-b} \quad [2]$$

$$205 \quad K = K_s \left( \frac{\theta}{\theta_s} \right)^{2b+2+p} \quad [3]$$

206 where  $\Psi_{soil}$  is the soil matric potential (kPa),  $a$  is the air entry water potential (kPa),  $b$  is  
 207 an empirically determined constant (-),  $\theta_s$  is the volumetric water content at saturation (%  
 208 vol.),  $\theta$  is the volumetric water content (% vol.),  $K$  is the hydraulic conductivity (mm day<sup>-1</sup>),  
 209  $K_s$  is the saturated hydraulic conductivity (mm day<sup>-1</sup>) and  $p$  is an interaction parameter  
 210 about pore size, the value of which is assumed to be 1 for the LEACHM model. A free-  
 211 draining lower boundary was assumed.

212 Although the objective of the work was not to assess the LEACHM model,  
 213 performance indicators were applied to validate simulations and detect anomalous data in  
 214 the standardization. Differences between observed values ( $\theta_{FDR}$ ) and predicted values  
 215 ( $\theta_{SIM}$ ) were evaluated by calculating two model evaluation indicators: i) the root mean  
 216 square error (RMSE) was selected for quantifying the error in terms of the units of the  
 217 variable calculated by the model and ii) the relative root mean squared error (RRMSE)  
 218 was used as indicator which is independent of the units of measurement. The minimum  
 219 value is 0, being also the optimal value (Loague and Green, 1991). Their definitions are  
 220 given by:

$$221 \quad RMSE = \sqrt{\frac{\sum_{i=1}^N (O_i - P_i)^2}{N}} \quad [4]$$

$$222 \quad RRMSE = \sqrt{\frac{\frac{1}{N} \sum_{i=1}^N (O_i - P_i)^2}{\bar{O}}} \quad [5]$$

223 where  $N$  is the number of measured data,  $O_i$  and  $P_i$  are the predicted and the measured  
224 values and  $\bar{O}$  is the mean of the observed values.

225 Indeed, the approach proposed in the present work offers an alternative methodology  
226 to traditional calibration that allows to simulate an unlimited number of water balances  
227 from soil samples. Certainly, this standardization methodology proposed could be  
228 replaced by any field or laboratory protocols to calibrate FDR sensors (Provenzano et al.,  
229 2015).

### 230 ***2.5. Critical soil water content extrapolation***

231 The  $\theta_{crit}$  should be adapted for scheduling mandarin irrigation under different soil  
232 physical conditions for instance by relating  $\Psi_{soil}$  and  $\theta$  using SWRCs. The SWRC allows  
233 transferring the  $\theta_{crit}$  from the conditions where they were obtained (Definition) to other  
234 locations (Validation) with different soil physical properties using the corresponding  $\Psi_{soil}$   
235 following these steps: i) to construct and to parameterize SWRCs for the surrounding soil  
236 where FDR probes were installed; ii) determination of the  $\Psi_{soil}$  corresponding to the  
237 critical soil water content of Definition FDR probes ( $\theta_{crit}^{Def}$ ); and iii) determination of the  
238 critical soil water content of Validation FDR probes ( $\theta_{crit}^{Val}$ ) corresponding to the  $\Psi_{soil}$   
239 obtained in the previous step.

240 Data for SWRC were generated using the pressure plate method (Richards, 1948),  
241 where  $\theta$  corresponding to  $\Psi_{soil}$  of 0, -10, -30, -60, -100, -300 and -1000 kPa was  
242 determined. Experimental data were fitted by means of the van Genuchten model (van  
243 Genuchten, 1980):

$$244 \quad \theta = \theta_r + \frac{\theta_s - \theta_r}{(1 + (\alpha \Psi_{soil})^n)^m} \quad [6]$$

245 where  $\theta$  is the soil water content (% vol.),  $\theta_r$  is the soil residual water content (% vol.),  $\theta_s$   
246 is the soil saturated water content (% vol.),  $\Psi_{soil}$  is the soil matric potential (kPa),  $\alpha$  is a

247 scale parameter inversely proportional to mean pore diameter ( $\text{cm}^{-1}$ ), and  $m$  and  $n$  are  
 248 parameters associated to the shape of the soil water characteristic curve being  $m=1-I \cdot n^{-1}$ .  
 249  $\theta_r$ ,  $\alpha$  and  $n$  could be calculated using a least squares objective function with certain  
 250 restrictions (Schaap et al., 1998; Anlauf, 2014):  $0.0 \leq \theta \leq 0.3 \text{ cm}^3 \text{ cm}^{-3}$ ;  $0.0001 \leq \alpha \leq 1.000$   
 251  $\text{cm}^{-1}$ , and  $1.001 \leq n \leq 10$ .

## 252 **2.5. Irrigation dose computation**

253 The aim of the sensor-based strategy was to restore water losses given by  
 254 evapotranspiration events and maintaining the soil moisture above the  $\theta_{crit}$ . Crop water  
 255 requirements were estimated according to crop evapotranspiration,  $ET_c$ , estimated with  
 256 the single crop coefficient approach (Allen et al., 1998).  $ET_0$  was determined with the  
 257 Penman - Monteith equation in the version modified by FAO (Allen et al., 1998), by using  
 258 the meteorological observations acquired by two automatic agro-meteorological stations  
 259 located nearby the orchard. The  $K_c$  varied among months depending on the crop  
 260 phenological stage. According to the canopy ground cover,  $K_c$  was assumed variable from  
 261 a minimum of 0.36 in May to a maximum of 0.56 in October (Castel, 2000). Irrigation  
 262 scheduling was programmed twice a week, Monday and Thursday.

263 The soil moisture was measured with the Validation FDR probes in the root profile  
 264 (0 - 0.5 m) before each scheduling event. Then, the irrigation required dose ( $V$ , mm) was  
 265 defined as:

$$266 \quad V = f_m \cdot z \cdot (\theta_{crit-FDR}^{Val} - \theta_{FDR}^{Val}) \quad [7]$$

267 where  $f_m$  (-) is the wetted soil fraction,  $z$  (mm) is the bulb depth,  $\theta_{FDR}^{Val}$  and  $\theta_{crit-FDR}^{Val}$   
 268 (%vol.) are the current and critical soil water content for scheduling irrigation with  
 269 Validation FDR probes, respectively. The total dose ( $V_t$ , mm) to be applied for  $i$  days and  
 270 the time for each irrigation event (IT, s) were calculated as:

271 
$$V_t = \sum_{i=1}^{i=n} CWR_i + V \quad [8]$$

272 
$$IT(S) = \frac{V_t \cdot S}{q_{intake} \cdot n} \quad [9]$$

273 where  $S$  (m<sup>2</sup>) is the total irrigated area,  $q_{intake}$  (L s<sup>-1</sup>) is the total flow delivered to the  
 274 subunit (irrigation area controlled by pressure regulator) and  $n$  (-) is the number of days  
 275 irrigation was performed for the scheduled interval.

276 **2.6. Irrigation strategy validation**

277 The sensor-based strategy was implemented during 2016 in the same experimental  
 278 plot where irrigation thresholds were obtained. The treatments applied were Control,  
 279 irrigated during the whole season at 100% ET<sub>c</sub> (Allen et al.,1998;Castel, 2000), and the  
 280 sensor-based strategy (SB strategy), irrigated following  $\theta_{crit}$ . For the strategy  
 281 implementation, the  $\theta_{crit}$  obtained from the stress cycles were extended to specific  
 282 developmental crop phenological stages of the trees with similar VPD levels: post-harvest  
 283 and bloom and fruit-set (Periods C1 and C2), phase I (Periods A1 and A2), phase II  
 284 (Periods B1 and B2) and phase III (Periods C1 and C2) of fruit growth.

285 The statistical design for comparing the two irrigation strategies was a randomized  
 286 complete block with three replicates per treatment. Each sub-plot had four rows with 6 -  
 287 7 sample trees per row where perimeter trees were used as guard, leaving 8 - 10 central  
 288 trees for experimental determinations.  $\Psi_{stem}$  was determined approximately weekly at  
 289 solar midday in two mature leaves of two trees per experimental unit for assessing plant  
 290 water status. In the SB strategy, FDR probes Validation 1 and 2 were used for measuring  
 291  $\theta$  and for scheduling irrigation. Yield was determined at the time of commercial harvest  
 292 in all the sampled trees. This was defined by the grower collaborator following the  
 293 standard fruit quality protocols used in the area. Juice total soluble solids content, juice  
 294 titratable acidity and maturity index about 12°Brix, 7 g/l and 17, respectively. According

295 to Perry et al., (2017), crop water productivity (CWP) was calculated as the crop yield  
296 divided by the irrigation volumes applied.

297

### 298 **3. Results and discussion**

#### 299 **3.1. Critical soil water content determination**

300 During the three drought cycles carried out in 2015 and 2016,  $\Psi_{Stem}$  and  $\theta_{FDR}$   
301 measured with Definition 1 to 4 FDR probes, were compared by using linear regressions  
302 (Figure 1). The equations depicted in Figure 1 are indicating the soil water status threshold  
303 below which  $\Psi_{Stem}$  do not decrease greatly in response to small changes in  $\theta$ . Differences  
304 among the slope of the curve can be observed for the different studied periods. This might  
305 be because of the variations in the VPD registered for each period. The most pronounced  
306 slopes were found in the summer stress cycles (periods B1 and B2), when VPD reached  
307 its maximum values (1.3 kPa) from DOY 201 to 207 in 2015. The most moderate slope  
308 was found from DOY 316 in 2015 to DOY 11 in 2016 (period C1), in agreement with  
309 low VPD (0.4 kPa), since the atmospheric demand is not a limiting factor and changes in  
310 the soil moisture do not result in drastic decreases in the plant water status. However,  
311 measurements from DOY 336 in 2016 to 13 in 2017 (period C2) showed a different trend  
312 with small variations in the  $\theta_{FDR}$  resulting in important changes in  $\Psi_{Stem}$ . Given the  
313 registered VPD values (0.2 kPa), this was an unexpected behavior. It could be a  
314 consequence of the low soil temperature probably occurring this winter period, which  
315 might have increased water viscosity and root hydraulic resistance hindering water  
316 absorption (Kramer, 1942; Runnin and Reid, 1980).

317 The linear equations that relate  $\Psi_{Stem}$  and  $\theta_{FDR}$  (Figure 1) were solved using the  
318  $\Psi_{Stem}$  thresholds proposed in the methodology. Results showed that the  $\theta_{crit-FDR}^{Def}$  for  
319 scheduling irrigation varied on the considered period of the year and the evaporative

320 demand (Table 3A). This is the main advantage of the proposed strategy because  
321 irrigation water needs are adapted to the soil water status and the crop phenological stage.  
322 It should be noted that the probes Definition 1 and 3 showed higher humidity values than  
323 the probes Definition 2 and 4. This fact may be attributed to the lack of calibration of the  
324 probes, to the soil characteristics, or even to the differences between plants.

### 325 **3.2. Critical soil water content standardization and extrapolation**

326 The simulation with LEACHM was performed for a cold period (from DOY 338 in  
327 2015 to 12 in 2016) without irrigation and with low evaporative demand, aiming to  
328 minimize the effect of the evapotranspiration rates on the soil water dynamics. Soil  
329 physical and chemical properties and crop data inputs are summarized in Tables 1 and 2.

330 Linear regression equations (Table 4) were calculated to consider differences  
331 between  $\theta_{FDR}$  and  $\theta_{SIM}$  and to standardize soil moisture values obtained with the FDR  
332 probes. The slope of the regression lines (a) give an idea of how well the simulation fits  
333 the real measurements. The slope of the regression varied between 0.67 to 1.03, indicating  
334 that data trends were reasonably similar and both methods were reproducing comparable  
335 soil water dynamics. The fitting constant b, that ranged between 2.68 and 15.63, showed  
336 the different levels of soil moisture provided by simulated and measured temporal series.  
337 For each probe,  $\theta_{FDR}$  was higher than  $\theta_{SIM}$  (data not shown). Other studies corroborate  
338 that electromagnetic soil water content sensors could overestimate volumetric water  
339 content due to presence of salt in soils (Sevostianova et al., 2015). Standardization  
340 equations were characterized by coefficients of determination ranging between 0.93 to  
341 0.72.

342 The standardization methodology was assessed by means of evaluation indicators.  
343 Errors were estimated with  $\theta_{SIM}$  and  $\theta_{FDR}$ . RMSE was  $1.0 \pm 0.4$  % vol. and RRMSE was  
344  $0.16 \pm 0.06$ . Both statistics are widely affected by the presence of outliers (Viteri, 2013),

345 and simulations performed with LEACHM model sometimes presented these punctual  
346 differences at the beginning of the simulated data set (data not shown). In other studies,  
347 the estimation of soil water content in the root zone was considered suitable when the  
348 RMSE was equal to 2.0 % vol. (Rallo et al., 2011), and the RRMSE was considered as  
349 valid when it was lower than 0.40 (Confalonieri and Bechini, 2004; Wallis at al., 2011).  
350 The soil water balance simulation with LEACHM, despite the difference with respect to  
351 the soil water content of the FDR, accurately reproduce moisture readings. This fact could  
352 lay the foundations for future research, where the  $\theta_{crit}$  may be used directly in the  
353 simulations, and thus, reduce the dependency of the equipment on continuous  
354 measurement of soil moisture.

355 There is no consensus in the scientific community regarding to capacitance probes  
356 calibration. Some authors ensure that FDR measurements are valid in any soil within wide  
357 ranges of soil moisture levels (Thomas, 1966; Hoekstra and Delaney, 1974). However,  
358 some studies have demonstrated that capacitance probes were influenced by the soil type  
359 (Bell et al., 1987). The proposed standardization, or any other analogous methodology, is  
360 indeed considering essential for ensuring the correct use of the SB strategy. Following  
361 this procedure, any volumetric water content value from FDR probe sensors could be  
362 adjusted at the same reference and data from different sensors could be comparable.

363 The  $\theta_{crit}^{Def}$  obtained by means of LEACHM standardization were 26.8, 28.9 and 24.4  
364 %vol. for periods A1 - A2, B1 - B2 and C1 - C2, respectively (Table 3B). A progressive  
365 increase of the values is recorded according to the VPD along the season. During the  
366 period B1 - B2 (summer), the  $\theta_{crit}^{Def}$  required to avoid plant stress was the highest, with 29  
367  $\pm 2\%$  vol., because of the high evaporative demand during this part of the season (VPD =  
368 1.2 kPa). The soil water storage capacity in this period should be enough for avoiding  
369 significant water stress (Girona et al., 2002). In contrast, the lowest  $\theta_{crit}^{Def}$  was determined



370 during the period C1- C2 (winter),  $24 \pm 3$  % vol. when the evaporative demand (VPD =  
371 0.3 kPa) is lower than in the summer. Indeed, the results showed that the critical soil water  
372 content to maintain an adequate plant water status was lower during periods of low-  
373 evaporative-demand as winter and the beginning of spring.

374 The seasonal weighted average  $\theta_{crit}^{Def}$  for the root profile (0 – 0.5 m) was 26 % vol.,  
375 similar to previous results obtained in grapefruit (Pérez-Pérez et al., 2008) and orange  
376 (Pérez-Pérez et al., 2014) irrigated at 100% ET<sub>c</sub>, with a volumetric soil water content in  
377 the entire soil profile (0 – 1 m) ranging between 21 and 25 % vol. and 24 and 24 % vol.,  
378 respectively. In these studies, volumetric soil water content was measured using a neutron  
379 probe previously calibrated at the experimental site. Differences could be attributed,  
380 among others, to the soil properties, measurement depth and citrus variety.

381 After applying the standardization process, extrapolation was made to adapt the  $\theta_{crit}^{Def}$   
382 to specific soil conditions where Validation 1 and 2 probes were installed. Extrapolated  
383  $\theta_{crit}^{Val}$  showed in the Table 5 have been classified in specific phenological stages (post-  
384 harvest, bloom and fruit-set and phase I, II and III of fruit growth ) in accordance with  
385 the registered average VPD during the drought cycles (Table 3) and during the season  
386 when the sensor-based strategy was implemented (Table 4). Indeed, the thresholds  
387 obtained for Validation probes were similar to the average values obtained for Definition  
388 probes probably because the soil homogeneity within the plot.

### 389 **3.3. Irrigation strategy validation**

390 Irrigation was scheduled by means of the sensor-based strategy during 2016 in the  
391 experimental plot using the Validation 1 and 2 FDR probes. The mean annual ET<sub>0</sub> and  
392 rainfall for the experimental season was of 1,122 and 716 mm, respectively. The temporal  
393 distribution of rainfall and VPD followed the typical patterns of the Mediterranean basin  
394 (Fig. 2A). The seasonal variation of rainfall was characterised by a period of great scarcity

395 during phase II of fruit growth (21 mm) and higher precipitation values were registered  
396 in the spring and the autumn, during bloom and fruit-set (113 mm) and phase III of fruit  
397 growth (548 mm). Mean daily VPD reached the highest values during phase II of fruit  
398 growth (1.1 kPa). During the implementation period (from January to November 2016),  
399 control trees received 581 mm of irrigation, while in the treatment irrigated following the  
400 SB strategy, the applied irrigation water was 429 mm (Fig. 2B). A 27 % water saving was  
401 achieved with the SB strategy, reaching the highest reductions (29%) during phase II of  
402 fruit growth.

403 These differences in water application resulted in slightly different plant water status  
404 between treatments (Fig. 2C). During post-harvest (DOY 11 and 21), the  $\Psi_{Stem}$   
405 registered in both treatments was lower than the thresholds established (-0.8 to -1.0 MPa)  
406 most likely because of the effect of low temperatures (12.4°C) which could reduce plant  
407 water uptake capacity. However, it should be noted that there were no statistically  
408 significant differences between the evaluated irrigation strategies. Later on, during the  
409 mid-winter period, plant water status was recovered in the control treatment because of  
410 the higher irrigation volume applied during the beginning of the crop season in  
411 comparisons with the SB strategy. During this period (DOY 33, 42 and 49), in the SB  
412 strategy  $\Psi_{Stem}$  was lower than -1.0 MPa with no statistically significant differences  
413 between irrigation strategies. From DOY 55, plant water status was recovered in both  
414 treatments, and specially since DOY 73 when pruning was made in the entire plot. During  
415 phase II of fruit growth (DOY 218, 232, 239 and 244),  $\Psi_{Stem}$  significantly decreased in  
416 the SB strategy, compared with control treatment. The plant water status values reached  
417 are probably consequence of the high evaporative demand during these periods. However,  
418 the threshold of -1.3 to -1.5 MPa established by Ballester et al. (2011 and 2014) and  
419 González-Altozano and Castel (1999) to avoid negative consequences in quality and yield

420 was not exceeded. During phase III of fruit growth (DOY 266 and 279) both treatments  
421 had an inadequate plant water status with the lowest values of  $\Psi_{stem}$  recorded in the SB  
422 strategy. The  $\theta_{crit}^{Val}$  used for this period was 24% vol. according to the low VPD registered  
423 in phase III of fruit growth (Table 5). However, final fruit growth and ripening took place  
424 and, even if the evaporative demand was low, the fruit sink demand for photoassimilates  
425 was elevated being the irrigation volumes applied probably insufficient. It would be  
426 desirable to increase the  $\theta_{crit}^{Val}$  for this stage, maintaining the levels of the phase II of fruit  
427 growth (29% vol.) until harvest. This fact underlines the importance of an appropriate  
428 determination and timing of the moisture thresholds.

429 Notwithstanding the water savings obtained in the SB strategy, no significant  
430 differences were found between treatments in terms of yield reaching  $73.3 \pm 23.2 \text{ kg tree}^{-1}$   
431 <sup>1</sup> and  $72.1 \pm 19.8 \text{ kg tree}^{-1}$  in control and SB strategy, respectively. These yield levels are  
432 well in line with the expected tree performance for mandarin trees in the area as reported  
433 in previous research (Ballester et al. 2014; Nicolas et al. 2016). The highest CWP was  
434 obtained in the SB strategy,  $7.2 \text{ kg m}^{-3}$ , compared to the control treatment,  $5.4 \text{ kg m}^{-3}$   
435 demonstrating that, the irrigation scheduling developed can optimize irrigation efficiency  
436 by better adjusting the watering regime to the actual orchard water consumption.  
437 Although there are other models for scheduling irrigation in citrus trees (Alba et al., 2003;  
438 Bonet et al. 2010), they do not consider the limits of moisture and its adaptation to other  
439 soils, two elements that are the basis of the model proposed. This work demonstrates that  
440 an irrigation schedule adjusted to the soil water content dynamics can improve the water  
441 use efficiency. However, irrigation time calculated by the proposed strategy should be  
442 monitored to avoid errors associated with FDR probe management. The small volume of  
443 soil sampled by FDR probes, the influence of air gaps or the lack of contact between  
444 sensors and soil may cause problems (Evetts and Parkin, 2005; Evetts et al., 2006). The

445 crop coefficient method for estimating water needs is too general and empiric, but it could  
446 be considered as a reference to compare results and reveal errors. Indeed, occasional  
447 determinations of plant water status could be also included in order to check if the  
448 irrigation scheduling regime is detrimentally affecting crop production.

449 Similar water savings with no yield reductions as observed in the present work were  
450 obtained in previous studies also in citrus trees using other irrigation strategies such as  
451 regulated deficit irrigation (RDI) (Ballester et al., 2014) and subsurface drip irrigation  
452 (Martínez-Gimeno et al., 2018). The SB strategy coupled with RDI strategies could be  
453 used to improve water productivity, reduce tree growth and improve fruit composition,  
454 enhancing thus economical profit (Pérez-Pérez et al., 2010). However, the SB strategy  
455 provide a  $\theta_{crit}$  considering an adequate  $\Psi_{Stem}$ , then future studies will be necessary to  
456 expand the scheduling range for conditions of greater stress in controlled deficit irrigation  
457 strategies. Moreover, the use of more paired  $\theta_{FDR}$  and  $\Psi_{Stem}$  measurements, not only  
458 restricted to the stress cycles tested, would substantially improve the determination of the  
459 critical soil water content thresholds.

460

#### 461 **4. Conclusions**

462 The determination and use of the  $\theta_{crit}$  is a useful tool for optimizing irrigation  
463 scheduling. The SB strategy computes the water doses considering the  $\theta_{FDR}$  and avoiding  
464 excessive depletions which may result in a too severe tree water stress. The strategy  
465 includes two steps for scheduling irrigation with FDR probes across mandarin orchards  
466 under similar climatic conditions. On the one hand, a standardization methodology  
467 minimizes sensor-to-sensor variations allowing to use absolute values of  $\theta_{crit}$  for  
468 estimating irrigation needs. On the other hand, an extrapolation methodology adapts  $\theta_{crit}$   
469 to any soil physical condition. The irrigation strategy was implemented in a commercial

470 orchard, and water savings reached 26% without limiting yield, thus increasing crop water  
471 productivity. Future work will be necessary for assessing the suitability of the proposed  
472 strategy in a multi-season study for different citrus varieties or species and under different  
473 crop conditions.

474

## 475 **5. Acknowledgements**

476 This experiment was funded by European project WEAM4i (Water & Energy Advanced  
477 Management for Irrigation), grant agreement 619061 and FEDER-MINECO projects  
478 EASYRIEGO (IPT-2012-0950-310000), RISUB (IPT-2012-0480-310000) and  
479 RIEGOTEL (RTC-2016-4972-2). M.A. Martínez-Gimeno acknowledges the financial  
480 support received from the Spanish Ministry of Education, Culture and Sports (MECD)  
481 program Formación Profesorado Universitario (FPU). Juan G. Pérez-Pérez also gratefully  
482 acknowledges the post-doctoral contract in the ‘Ramón y Cajal’ program, supplied by the  
483 Spanish Ministry of Economy, Industry and Competitiveness (MINECO). Authors would  
484 like to thank M. Jordà, C. Albert, F. Sanz and A. Yeves for the support on installation and  
485 maintenance of the equipment. Thanks also to Prof. G. Provenzano (University of  
486 Palermo) for his critical comments and suggestions.

487

## 488 **6. References**

489 Aboutatallah, A., Salghi, R., El Fadl, A., Hammouti, B., Zarrouk, A., 2012. Shading nets  
490 usefulness for water saving on citrus orchards under different irrigation doses.  
491 Current World Environment, 7,1, 13.

492 Alba, I., Rodrigues, P. N., Pereira, L. S., 2003. Irrigation scheduling simulation for citrus  
493 in Sicily to cope with water scarcity. In *Tools for Drought Mitigation in*  
494 *Mediterranean Regions*. Springer, Dordrecht, pp. 223-242.

495 Allen, R. G., Pereira, L. S., Raes, D., Smith, M., 1998. FAO Irrigation and drainage paper  
496 No. 56. Rome: Food and Agriculture Organization of the United Nations, 56-97.

497 Alva, A. K., Paramasivam, S., Fares, A., Obreza, T. A., Schumann, A. W., 2006. Nitrogen  
498 best management practice for citrus trees: II. Nitrogen fate, transport, and  
499 components of N budget. *Scientia Horticulturae*, 109, 3, 223-233.

500 Anlauf, R., 2014. Using the EXCEL solver function to estimate the van Genuchten  
501 parameters from measured pF/water content values (accessed 12 December 2015).

502 Asada, K., Eguchi, S., Urakawa, R., Itahashi, S., Matsumaru, T., Nagasawa, T., Katou,  
503 H., 2013. Modifying the LEACHM model for process-based prediction of nitrate  
504 leaching from cropped Andosols. *Plant and soil*, 373(1-2), 609-625.

505 Autovino, D., Rallo, G., Provenzano, G., 2018. Predicting soil and plant water status  
506 dynamic in olive orchards under different irrigation systems with Hydrus-2D:  
507 Model performance and scenario analysis. *Agricultural Water Management*, 203,  
508 225-235.

509 Ballester, C., Castel, J., Intrigliolo, D. S., Castel, J. R., 2011. Response of Clementina de  
510 Nules citrus trees to summer deficit irrigation. Yield components and fruit  
511 composition. *Agricultural Water Management*, 98(6), 1027-1032.

512 Ballester, C., Castel, J., El-Mageed, T. A., Castel, J. R., Intrigliolo, D. S., 2014. Long-  
513 term response of 'Clementina de Nules' citrus trees to summer regulated deficit  
514 irrigation. *Agricultural Water Management*, 138, 78-84.

515 Bell, J. P., Dean, T. J., Hodnett, M. G., 1987. Soil moisture measurement by an improved  
516 capacitance technique, Part II. Field techniques, evaluation and calibration.  
517 Journal of Hydrology, 93(1-2), 79-90.

518 Bonet, L., Ferrer, P.J., Castel, J.R., Intrigliolo, D.S., 2010. Soil capacitance sensors and  
519 stem dendrometers: useful tools for irrigation scheduling of commercial orchards?  
520 Spanish Journal of Agricultural Research, 2, 52-65

521 Campbell, G. S., 1974. A simple method for determining unsaturated conductivity from  
522 moisture retention data. Soil Science, 117,6, 311-314.

523 Campbell, G. S., Campbell, M. D., 1982. Irrigation scheduling using soil moisture  
524 measurements: theory and practice. Advances in irrigation, 1, 25-42.

525 Castel, J.R., 2000. Water use of developing citrus canopies in Valencia, Spain. In: Proc  
526 Int. Soc. Citriculture IX Congr., pp. 223–226.

527 Childs, S., Hanks, R. J., 1975. Model of Soil Salinity Effects on Crop Growth 1. Soil  
528 Science Society of America Journal, 39(4), 617-622.

529 Confalonieri, R., Bechini, L., 2004. A preliminary evaluation of the simulation model  
530 CropSyst for alfalfa. European Journal of Agronomy, 21(2), 223-237.

531 Consoli, S., O'Connell, N., Snyder, R., 2006. Measurement of light interception by navel  
532 orange orchard canopies: case study of Lindsay, California. Journal of Irrigation  
533 and Drainage Engineering, 132(1), 9-20.

534 Deng, Z., Guan, H., Hutson, J., Forster, M. A., Wang, Y., Simmons, C. T., 2017. A  
535 vegetation-focused soil-plant-atmospheric continuum model to study  
536 hydrodynamic soil-plant water relations. Water Resources Research, 53(6), 4965-  
537 4983.

538 Evett, S. R., Parkin, G. W., 2005. Advances in soil water content sensing. Vadose Zone  
539 Journal, 4(4), 986-991.

540 Evett, S. R., Tolk, J. A., Howell, T. A., 2006. Soil profile water content determination:  
541 Sensor accuracy, axial response, calibration, temperature dependence, and  
542 precision. *Vadose Zone J.*, 5,3, 894–907.

543 Evett, S.R., Ruthardt, B.B., Kottkamp, S.T., Howell, T.A., Schneider, A.D., Tolk, J.A.,  
544 2002. Accuracy and precision of soil water measurements by neutron,  
545 capacitance, and TDR methods, in: *Proceedings of the 17th Water Conservation*  
546 *Soil Society Symposium, Thailand.*

547 Fares, A., Polyakov, V., 2006. Advances in crop water management using capacitive  
548 water sensors. *Advances in Agronomy*, 90, 43-77.

549 Fereres, E., Soriano, M. A., 2006. Deficit irrigation for reducing agricultural water use.  
550 *Journal of experimental botany*, 58(2), 147-159.

551 García-Tejero, I., Durán-Zuazo, V. H., Muriel-Fernández, J. L., Martínez-García, G.,  
552 Jiménez-Bocanegra, J. A., 2011. Benefits of low-frequency irrigation in citrus  
553 orchards. *Agronomy for Sustainable Development*, 31(4), 779.

554 Girona, J., Mata, M., Fereres, E., Goldhamer, D. A., Cohen, M., 2002. Evapotranspiration  
555 and soil water dynamics of peach trees under water deficits. *Agricultural Water*  
556 *Management*, 54,2, 107-122.

557 González-Altozano, P., Castel, J. L., 1999. Effects of regulated deficit irrigation on  
558 Clementina de Nules citrus trees growth, yield and fruit quality. In *III International*  
559 *Symposium on Irrigation of Horticultural Crops 537*, pp. 749-758.

560 Hignett, C., Evett, S., 2008. Direct and surrogate measures of soil water content. *Field*  
561 *estimation of soil water content: A practical guide to methods, instrumentation,*  
562 *and sensor technology*, S. R. Evett, L. K. Heng, P. Moutonnet, and M. L. Nguyen,  
563 eds., International Atomic Energy Agency, Vienna, Austria.



564 Hoekstra, P., Delaney, A., 1974. Dielectric properties of soils at UHF and microwave  
565 frequencies. *Journal of Geophysical Research*, 79, 11, 1699-1708.

566 Hutson, J. L., Cass, A., 1987. A retentivity function for use in soil–water simulation  
567 models. *Journal of Soil Science*, 38, 1, 105-113.

568 Hutson, J.L., 2003. LEACHM – Leaching Estimation and Chemistry Model. Department  
569 of Crop and Soil Sciences. Cornell University, Ithaca, New York.

570 Instituto Geográfico Nacional. Ministerio de Fomento, IGN., 2018. Atlas Nacional de  
571 España. España en mapas. Una síntesis geográfica. Mapa Evapotranspiración.  
572 AEMET. Período 1996-2016.

573 Kramer, P. J. (1942). Species differences with respect to water absorption at low soil  
574 temperatures. *American Journal of Botany*, 29(10), 828-832.

575 Lidón, A., Ramos, C., Rodrigo, A., 1999. Comparison of drainage estimation methods in  
576 irrigated citrus orchards. *Irrigation science*, 19(1), 25-36.

577 Lidón, A., Ramos, C., Ginestar, D., Contreras, W., 2013. Assessment of LEACHN and a  
578 simple compartmental model to simulate nitrogen dynamics in citrus orchards.  
579 *Agricultural Water Management*, 121, 42-53.

580 Loague, K., Green, R. E., 1991. Statistical and graphical methods for evaluating solute  
581 transport models: overview and application. *Journal of Contaminant Hydrology*,  
582 7(1-2), 51-73.

583 Martínez-Gimeno, M. A., Bonet, L., Provenzano, G., Badal, E., Intrigliolo, D. S.,  
584 Ballester, C., 2018. Assessment of yield and water productivity of clementine  
585 trees under surface and subsurface drip irrigation. *Agricultural Water*  
586 *Management*, 206, 209-216.

587 Menenti, M., Alfieri, S.M., Bonfante, A., Riccardi, M., Basile, A., Monaco, E., Michele,  
588 C.D. Lorenzi, F.D., 2013. Adaptation of Irrigated and Rainfed Agriculture to

589 Climate Change: The Vulnerability of Production Systems and the Potential of  
590 Intraspecific Biodiversity (Case Studies in Italy), in: Filho, W.L. (Ed.), Handbook  
591 of Climate Change Adaptation. Springer Berlin Heidelberg, pp. 1–35.

592 Milano, M., Ruelland, D., Fernandez, S., Dezetter, A., Fabre, J., Servat, E., Fritsch, J.-  
593 M., Ardoin-Bardin, S., Thivet, G., 2013. Current state of Mediterranean water  
594 resources and future trends under climatic and anthropogenic changes.  
595 Hydrological Sciences Journal, 58(3), 498-518.

596 Minacapilli, M., Iovino, M., D'Urso, G., 2008. A distributed agro-hydrological model for  
597 irrigation water demand assessment. Agricultural Water Management, 95, 123-  
598 132.

599 Moriana, A., Pérez-López, D., Prieto, M. H., Ramírez-Santa-Pau, M., Pérez-Rodríguez,  
600 J. M., 2012. Midday stem water potential as a useful tool for estimating irrigation  
601 requirements in olive trees. Agricultural Water Management, 112, 43-54.

602 Muñoz-Carpena, R., Shukla, S., Morgan, K., 2004. Field devices for monitoring soil  
603 water content (Vol. 343, pp. 1-24). University of Florida Cooperative Extension  
604 Service, Institute of Food and Agricultural Sciences, EDIS.

605 Nasri, N., Chebil, M., Guellouz, L., Bouhlila, R., Maslouhi, A., Ibnoussina, M., 2015.  
606 Modelling nonpoint source pollution by nitrate of soil in the Mateur plain,  
607 northeast of Tunisia. Arabian Journal of Geosciences, 8, 1057-1075.

608 Nicolas, E., Alarcón, J.J., Mounzer, O., Pedrero, F., Nortes, P.A., Alcobendas, R.,  
609 .Romero-Trigueros, C., Bayona, J.M., Maestre-Valero, J.F. 2016. Long-term  
610 physiological and agronomic responses of mandarin trees to irrigation with saline  
611 reclaimed water. Agricultural Water Management, 166, 1-8.

612 Nimah, M. N., Hanks, R. J., 1973. Model for Estimating Soil Water, Plant, and  
613 Atmospheric Interrelations: I. Description and Sensitivity 1. Soil Science Society  
614 of America Journal, 37(4), 522-527.

615 Paraskevas, C., Georgiou, P., Ilias, A., Panoras, A., Babajimopoulos, C., 2012.  
616 Calibration equations for two capacitance water content probes in a Lysimeter  
617 field. *Int. Agrophys.*, 26(3), 285–293

618 Pérez, F., 2016. Programación de riego y déficit hídrico controlado en frutales de hueso.  
619 (Doctoral dissertation, Universidad Politécnica de Cartagena).

620 Pérez-Pérez, J. G., Romero, P., Navarro, J. M., Botía, P., 2008. Response of sweet orange  
621 cv ‘Lane late’ to deficit irrigation in two rootstocks. I: water relations, leaf gas  
622 exchange and vegetative growth. *Irrigation Science*, 26(5), 415-425.

623 Pérez-Pérez, J. G., García, J., Robles, J. M., Botía, P., 2010. Economic analysis of navel  
624 orange cv. ‘Lane late’ grown on two different drought-tolerant rootstocks under  
625 deficit irrigation in South-eastern Spain. *Agricultural Water Management*, 97(1),  
626 157-164.

627 Pérez-Pérez, J. G., Robles, J. M., Botía, P., 2014. Effects of deficit irrigation in different  
628 fruit growth stages on ‘Star Ruby’ grapefruit trees in semi-arid conditions.  
629 *Agricultural water management*, 133, 44-54.

630 Perry, C., Steduto, P., Karajeh, F., 2017. Does improved irrigation technology save water?  
631 A review of the evidence. Food and Agriculture Organization of the United  
632 Nations, Cairo, 42.

633 Provenzano, G., Rallo, G., Ghazouani, H., 2015. Assessing field and laboratory  
634 calibration protocols for the diviner 2000 probe in a range of soils with different  
635 textures. *Journal of Irrigation and Drainage Engineering*, 142(2), 04015040.

636 Quiñones, A., Martínez-Alcántara, B., Legaz, F., 2007. Influence of irrigation system and  
637 fertilization management on seasonal distribution of N in the soil profile and on  
638 N-uptake by citrus trees. *Agriculture, Ecosystems and Environment*, 122(3), 399-  
639 409.

640 Rallo, G., Agnese, C., Minacapilli, M., Provenzano, G., 2011. Comparison of SWAP and  
641 FAO agro-hydrological models to schedule irrigation of wine grapes. *Journal of*  
642 *Irrigation and Drainage Engineering*, 138(7), 581-591.

643 Ramos, C., Carbonell, E. A., 1991. Nitrate leaching and soil moisture prediction with the  
644 LEACHM model. *Fertilizer Research*, 27(2-3), 171-180.

645 Richards, L. A., 1931. Capillary conduction of liquids through porous mediums. *Physics*,  
646 1(5), 318-333.

647 Richards, L.A., 1948. Porous plate apparatus for measuring moisture retention and  
648 transmission by soil. *Soil Science*, 66, 105–110.

649 Ruiz Sánchez, M. C., Domingo Miguel, R., Castel Sánchez, J. R., 2010. Deficit irrigation  
650 in fruit trees and vines in Spain: a review. *Spanish Journal Agricultural Research*,  
651 8 (2), 5–20

652 Running, S. W., Reid, C. P., 1980. Soil temperature influences on root resistance of *Pinus*  
653 *contorta* seedlings. *Plant physiology*, 65(4), 635-640.

654 Schaap, M. G., Leij, F. J., Van Genuchten, M. T., 1998. Neural network analysis for  
655 hierarchical prediction of soil hydraulic properties. *Soil Science Society of*  
656 *America Journal*, 62(4), 847-855.

657 Sevostianova, E., Deb, S., Serena, M., VanLeeuwen, D., Leinauer, B. 2015. Accuracy of  
658 two electromagnetic soil water content sensors in saline soils. *Soil Science Society*  
659 *of America Journal*, 79(6), 1752-1759.

660 Soil Survey Staff, 1975. Soil taxonomy: a basic system of soil classification for making  
661 and interpreting soil surveys. United States Department of Agriculture, Soil  
662 Conservation Service.

663 Spinelli, G.M., Shackel, K.A., Gilbert, M. E., 2017. A model exploring whether the  
664 coupled effects of plant water supply and demand affect the interpretation of water  
665 potentials and irrigation management. *Agricultural. Water Management*, 192,  
666 271–280.

667 Syvertsen, J. P., Goñi, C., Otero, A., 2003. Fruit load and canopy shading affect leaf  
668 characteristics and net gas exchange of ‘Spring’ navel orange trees. *Tree*  
669 *Physiology*, 23(13), 899-906.

670 Thomas, A. M., 1966. In situ measurement of moisture in soil and similar substances by  
671 “fringe” capacitance. *Journal of Scientific Instruments*, 43(1), 21.

672 Turner, N.C., 1981. Techniques and experimental approaches for the measurement of  
673 plant water status. *Plant. Soil*, 58 (1–3), 339–366.

674 Van Genuchten, M. T., 1980. A closed-form equation for predicting the hydraulic  
675 conductivity of unsaturated soils 1. *Soil Science Society of America Journal*,  
676 44(5), 892-898.

677 Viteri, L. O., 2013. Ajuste, validación y aplicación del modelo EU-Rotate\_N en una zona  
678 vulnerable a la contaminación por nitratos. Optimización de la fertilización  
679 nitrogenada (Doctoral dissertation, Universidad de La Rioja).

680 Walkley, A., Black, I. A., 1934. An examination of the Degtjareff method for determining  
681 soil organic matter, and a proposed modification of the chromic acid titration  
682 method. *Soil Science*, 37(1), 29-38.

683 Wallis, K.L., Candela, L., Mateos, R.M., Tamoh, K., 2011. Simulation of nitrate leaching  
684 under potato crops in a mediterranean area. Influence of frost prevention irrigation  
685 on nitrogen transport. *Agricultural Water Management*. 98, 1629-1640.

686 Yonemoto, Y., Matsumoto, K., Furukawa, T., Asakawa, M., Okuda, H., Takahara, T.,  
687 2004. Effects of rootstock and crop load on sap flow rate in branches of  
688 ‘Shirakawa Satsuma’mandarin (*Citrus unshiu* Marc.). *Scientia Horticulturae*,  
689 102(3), 295-300.

690 Zhang, K., Greenwood, D. J., Spracklen, W. P., Rahn, C. R., Hammond, J. P., White, P.  
691 J., Burns, I. G., 2010. A universal agro-hydrological model for water and nitrogen  
692 cycles in the soil–crop system SMCR\_N: Critical update and further validation.  
693 *Agricultural Water Management*, 97(10), 1411-1422.

694

695 **Table 1.** Summary of the soil physical properties and crop data as inputs for the LEACHM  
 696 model.

697

Component	Parameter	Units	Value
Soil profile data	Soil bulk density	kg dm <sup>-3</sup>	See table 2
	Clay	%	See table 2
	Silt	%	See table 2
	Organic carbon	%	See table 2
	Particle density (clay, silt and sand)	kg dm <sup>-3</sup>	See table 2
	Exponent for Campbell's equation	-	See table 2
	Hydraulic conductivity	mm d <sup>-1</sup>	See table 2
	Particle density (clay, silt and sand)	kg dm <sup>-3</sup>	2.65
	Particle density (organic matter)	kg dm <sup>-3</sup>	1.10
	Wilting point	kPa	-1500
Crop data	Maximum ratio of actual to potential T	-	1.1
	Minimum root water potential	kPa	-3000
	Root resistance	-	1
	Crop cover fraction	-	1
	Pan factor	-	1.50
Weather data	Rain	mm	Daily data
	Potential evapotranspiration	mm	Weekly totals
	Temperature	°C	Mean weekly
	Thermal amplitude	°C	Mean weekly

698

699

700 **Table 2.** Soil physical and chemical properties for the different soils where FDR probes were  
 701 installed.

702

Parameter	Reference				Scheduling	
	1	2	3	4	1	2
Soil bulk density (kg dm <sup>-3</sup> )	1.53	1.54	1.56	1.49	1.55	1.58
Clay (%)	28.0	29.0	26.0	24.0	25.4	24.7
Silt (%)	35.5	35.5	36.0	39.0	39.9	39.8
Organic carbon (%)	0.48	0.52	0.44	0.62	0.54	0.54
Air entry value (kPa)	-0.33	-0.72	-0.75	-0.66	-2.51	-2.23
Exponent for Campbell's equation (-)	12.00	12.00	11.31	11.59	7.49	11.15
Hydraulic conductivity (mm d <sup>-1</sup> )	99.48	37.20	59.04	111.72	118.68	95.52

703

704

705

706

707

708

709 **Table 3.** (A) Critical soil water content measured by FDR probes ( $\theta_{crit-FRD}^{Def}$ ), and (B)  
 710 standardized critical soil water content ( $\theta_{crit}^{Def}$ ) for probes noted as Definition 1 to 4 obtained from  
 711 solving linear regressions from Figure 1. Average vapour deficit pressure (VPD) is indicated for  
 712 each period.

713

	Period A1 - A2	Period B1 - B2	Period C1 - C2
	VPD = 0.9 - 1.1 kPa	VPD = 1.1 - 1.3 kPa	VPD = 0.2 - 0.4 kPa
<b>A) Critical soil water content measured by FDR probes, <math>\theta_{crit-FRD}^{Def}</math> (% vol.)</b>			
Definition 1	34.1	36.2	33.6
Definition 2	31.7	33.2	30.3
Definition 3	33.6	35.3	30.5
Definition 4	31.3	33.6	28.2
<b>B) Standardized critical soil water content, <math>\theta_{crit}^{Def}</math> (% vol.)</b>			
Definition 1	26.6	28.9	26.0
Definition 2	28.2	29.6	26.8
Definition 3	24.9	26.8	21.4
Definition 4	27.3	30.3	23.4
$\mu$	26.8	28.9	24.4
$\sigma$	1.4	1.5	2.5

714

715

716 **Table 4.** Fitting linear regression equations between volumetric soil water content measured by  
 717 means FDR probes ( $\theta_{FDR}$ ) and simulated with LEACHM model ( $\theta_{SIM}$ ) for Definition (1 to 4) and  
 718 Validation (1 to 2) FDR probes. Constants a and b are the fitting parameters and Rsqr is the  
 719 coefficient of determination.

720

	$\theta_{FDR} = a \theta_{SIM} + b$		
	a	b	Rsqr
Definition 1	0.89	10.45	0.90
Definition 2	1.03	2.68	0.93
Definition 3	0.91	11.00	0.82
Definition 4	0.78	9.97	0.90
Validation 1	0.69	15.63	0.72
Validation 2	0.67	14.62	0.84



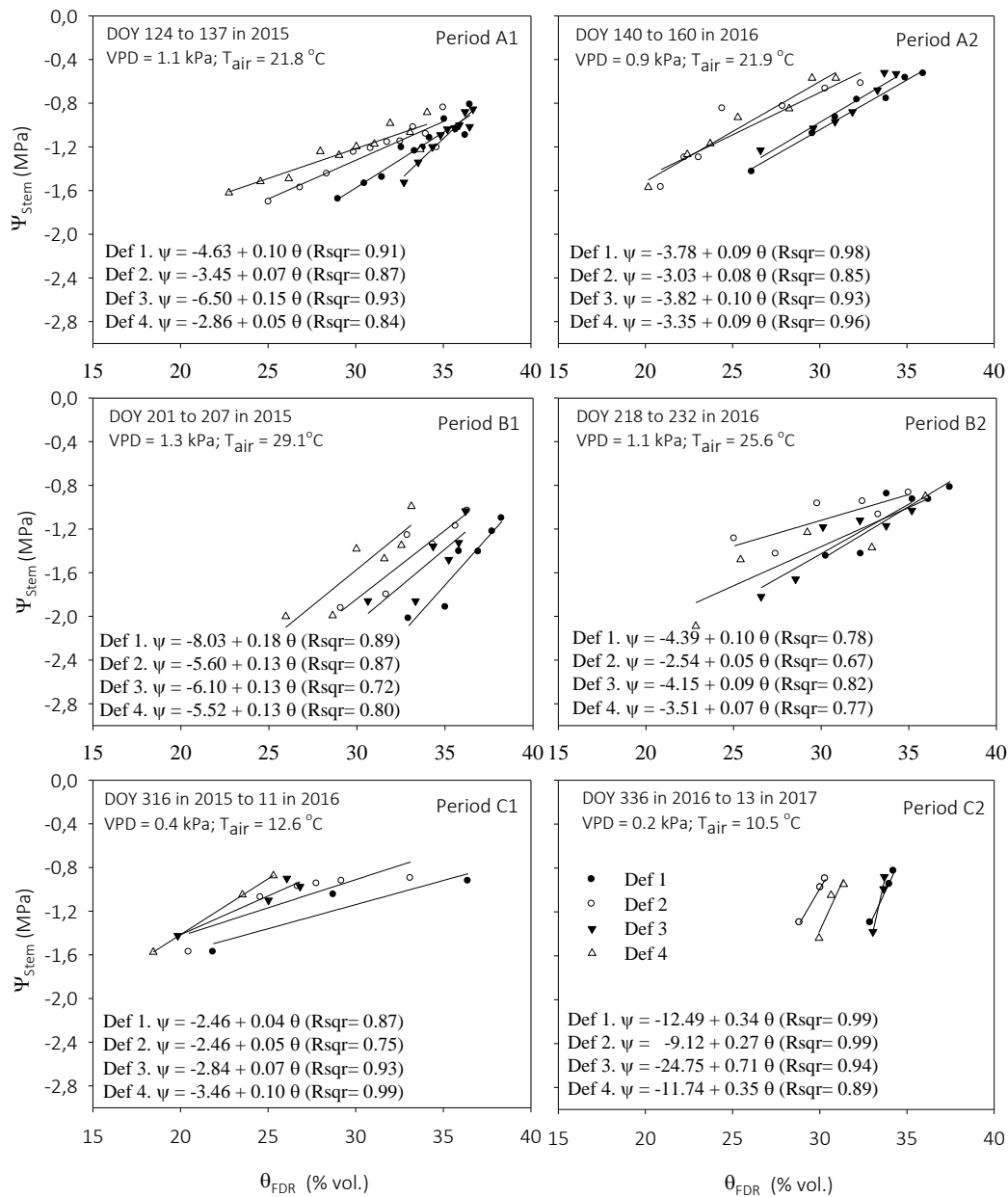
721 **Table 5.** (A) Critical soil water content for scheduling irrigation by FDR probes ( $\theta_{crit-FRD}^{val}$ ) and  
 722 (B) standardized critical soil water content for scheduling irrigation ( $\theta_{crit}^{val}$ ) for probes noted as  
 723 Validation 1 and 2 for post-harvest, bloom and fruit-set and phases I II and III of fruit growth.  
 724 Average vapour deficit pressure (VPD) is indicated for each phase.

725

	Post-harvest VPD = 0.6kPa	Bloom and fruit set VPD = 0.6 kPa	Phase I VPD = 0.9 kPa	Phase II VPD = 1.1 kPa	Phase III VPD = 0.5 kPa
<b>A) Critical soil water content measured by FDR probes, <math>\theta_{crit-FRD}^{val}</math> (% vol.)</b>					
Validation 1	32.2	32.2	33.9	35.5	32.2
Validation 2	30.3	30.3	31.9	33.5	30.3
<b>B) Standardized critical soil water content, <math>\theta_{crit}^{val}</math> (% vol.)</b>					
Validation 1	24.0	24.0	26.5	28.8	24.0
Validation 2	23.4	23.4	25.8	28.1	23.4
$\mu$	23.7	23.7	26.2	28.5	23.7
$\sigma$	0.4	0.4	0.5	0.5	0.4

726

727



729

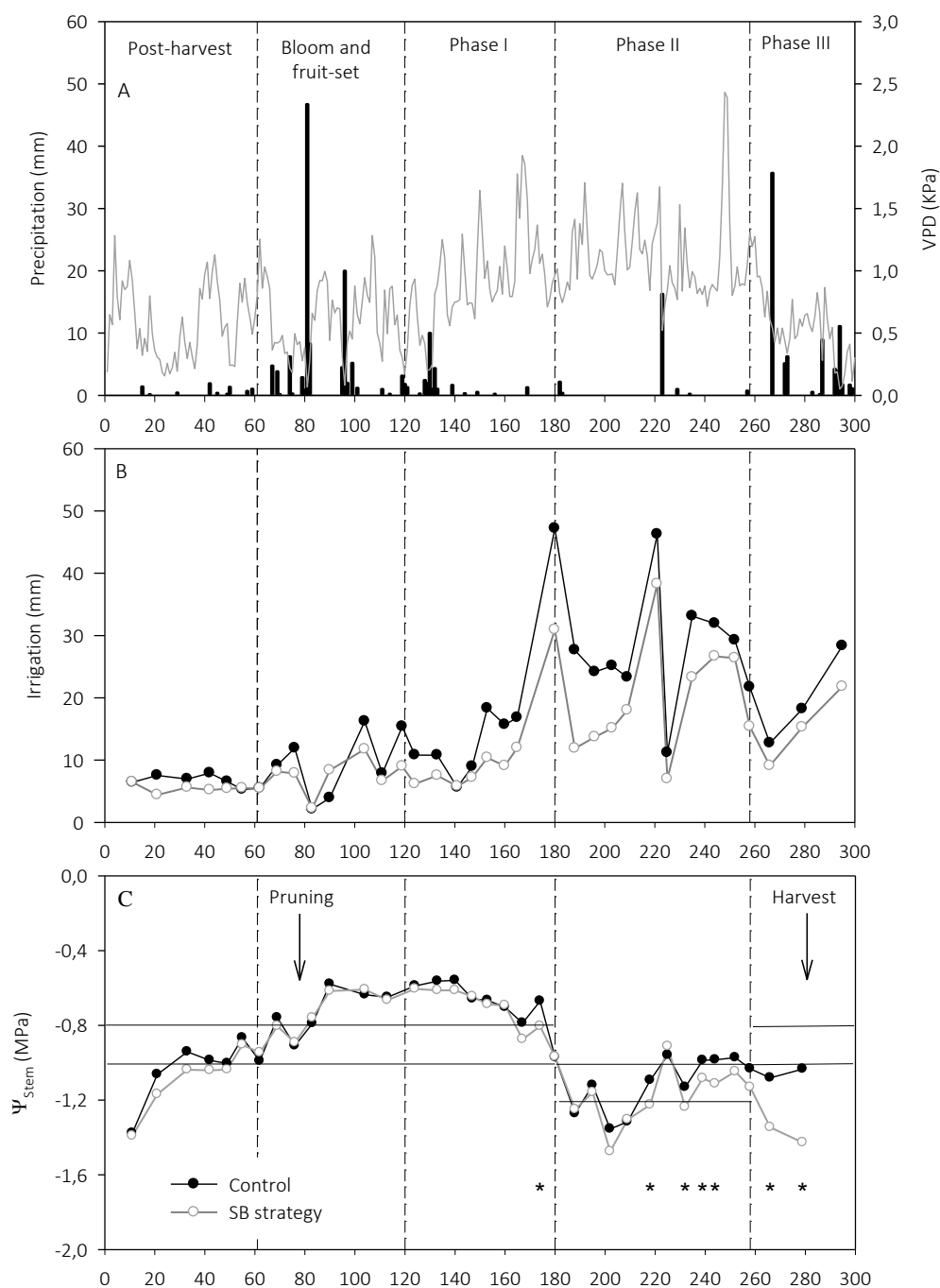
730 **Fig. 1.** Experimental values of midday stem water potential ( $\Psi_{Stem}$ ) and its corresponding soil  
 731 water content measured with FDR probes ( $\theta_{FDR}$ ) in the layer 0.2 – 0.5 m obtained from the  
 732 drought cycles made in 2015 and 2016. Def. refers to the four FDR probes used for measuring  
 733 soil water content. Linear regression and coefficient of determination (Rsqr) for each repetition  
 734 are represented. Day of the year (DOY), average air temperature ( $T_{air}$ ) and average air vapour  
 735 pressure deficit (VPD) is indicated for each graph.

736

737

738

739



740

741 **Fig. 2.** Seasonal patterns of (A) mean daily air vapour deficit pressure (VPD; solid line) and  
 742 precipitation (vertical bars); and (B and C) irrigation depths and midday stem water potential  
 743 ( $\Psi_{stem}$ ) in each treatment [control and sensor-based (SB) strategy] during 2016. Control  
 744 treatment was irrigated during the whole season at 100%  $ET_c$  and the SB strategy was irrigated  
 745 following soil water content measured with FDR probes. In C, horizontal lines show the  
 746 thresholds of  $\psi_{stem}$  used to evaluate plant water status; and asterisks represent statistically  
 747 significant differences in  $\psi_{stem}$  at  $P < 0.05$  between treatments. Vertical dotted lines show post-  
 748 harvest, bloom and fruit-set and fruit growth phases (I, II and III). Arrows in figure (C) indicate  
 749 the pruning and harvest date.

750